Energy 93 (2015) 994–998

Contents lists available at ScienceDirect

Energy

journal homepage: www.elsevier.com/locate/energy

Effect of coupling position on a looped three-stage thermoacoustically-driven pulse tube cryocooler

Jingyuan Xu [a, b], Jianying Hu [a, **], Limin Zhang [a], Wei Dai [a], Ercang Luo [a, *]

[a] Key Laboratory of Cryogenics, Technical Institute of Physics and Chemistry, Chinese Academy of Sciences, Beijing 100190, China
[b] Chinese Academy of Sciences, Beijing 100190, China

ARTICLE INFO

Article history:
Received 17 May 2015
Received in revised form
22 August 2015
Accepted 22 September 2015
Available online 22 October 2015

Keywords:
Thermoacoustically-driven cryocooler
Looped traveling-wave heat engine
Pulse tube cryocooler
Coupling mechanism

ABSTRACT

A looped three-stage thermoacoustically-driven cryocooler system is introduced. Based on classic thermoacoustic theory, simulations are performed to investigate the effects of three representative coupling positions (inlet, middle, and outlet) of the resonance tube. The total exergy efficiency is found to depend on the dimensions of the resonance tube, demonstrating the importance of this parameter. For the same resonance tube length, the highest exergy efficiency of 16.3% is achieved for the outlet coupling position, whereas the middle and inlet coupling positions only achieved highest exergy efficiencies of 9% and 14.93%, respectively. The distribution of the phase difference, acoustic power, and exergy loss ratios of the main components are then presented to clarify the coupling mechanism. The results show that better phase distribution in the regenerator and less exergy loss in the resonance tube contribute significantly to the superior performance of the outlet coupling position.

1. Introduction

THE (Thermoacoustic heat engines) and PTC (pulse tube coolers) have attractive application potential because of their mechanical simplicity and high reliability. Using the acoustic power spontaneously generated by the THE to drive the PTC results in a so-called thermoacoustically-driven cooling system with no moving mechanical components. The first thermoacoustically-driven system, developed in 1990, was capable of reaching a temperature of 90 K [1]. Since then, many efforts have been made to improve the performance of such systems and some important advances have been achieved [2–5]. However, most of the reported thermoacoustically-driven systems have two drawbacks: one is their non-compact size and shape, which incorporates a long and large-diameter standing-wave resonance tube; the other is substantial dissipation of acoustic power in the resonance tube, leading to low efficiency. In 2010, De Blok developed a four-stage looped traveling-wave THE, providing a possible solution to the problem [6]. Owing to its compact size and potential high efficiency, the looped multi-stage thermoacoustic system has been a focus of research ever since [7–9]. Fig. 1 shows a schematic of the three-stage system investigated in the present study. Following a theoretical analysis of its performance and mechanism, our research group conducted preliminary experiments on the looped three-stage cooling system and obtained a total exergy efficiency of 3.5% [10]. Later, an improved version achieved a total exergy efficiency of approximately 8% and a cooling capacity of more than 1 kW at 130 K [11], presenting exciting prospects for applications such as natural gas liquefaction and recondensation.

In Fig. 1, the acoustic power generated by the engine flows from one end of the resonance tube to the other. Simply considered, the PTC may be connected to any location of the resonance tube; however, owing to the strong acoustic characteristics of the system, the connection position affects the acoustic field both up- and downstream. The manner in which the coupling position affects the system performance remains a subject for further study. The present paper numerically investigates three representative coupling positions, as shown in Fig. 1: the inlet of the resonance tube (IR-coupling), the middle of the resonance tube (MR-coupling), and the outlet of the resonance tube (OR-coupling), which are all defined according to the direction of the acoustic power flow. The simulations firstly evaluate the effect of the dimensions of the resonance tube on system performance. Using the optimal dimensions of the resonance tube for each coupling position, the phase difference,

* Corresponding author. Tel./fax: +86 10 82543750.
** Corresponding author. Tel./fax: +86 10 82543733.
E-mail addresses: jyhu@mail.ipc.ac.cn (J. Hu), Ecluo@mail.ipc.ac.cn (E. Luo).

http://dx.doi.org/10.1016/j.energy.2015.09.099
0360-5442/

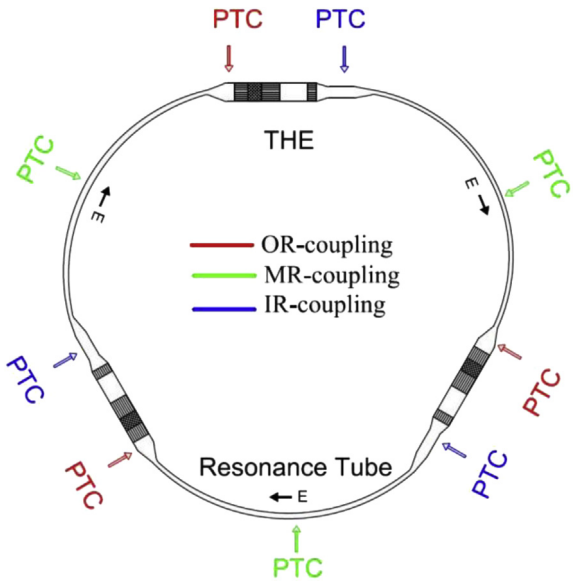

Fig. 1. Schematic view of the acoustically resonant cooling system.

acoustic power, and exergy loss are then investigated to clarify the performance differences. Finally, conclusions are given.

2. Numerical simulation and analysis

2.1. Looped three-stage thermoacoustically-driven cryocooler

Although there is no theoretical limit on the number of subunits, a three-stage system was chosen as a typical example here, based on a compromise between considerations of the total power scale and the efforts required in the construction of the experiments. As mentioned above, we have carried out several theoretical and experimental studies of the three-stage system and have achieved some progress, which inspired us to further investigate such systems. Fig. 1 shows the system configuration with three different PTC connection positions. Fig. 2 presents an enlarged view of one of the three identical subunits, which includes a THE and a PTC. The THE includes two water-cooled ambient heat exchangers, a regenerator, a heater block, a thermal buffer tube, and a resonance tube. The PTC includes an ambient heat exchanger, a regenerator, a cold head, a pulse tube, flow straighteners, and a phase shifter (comprising an inertance tube and a gas reservoir). Dimensions of the THE and PTC are presented in Table 1.

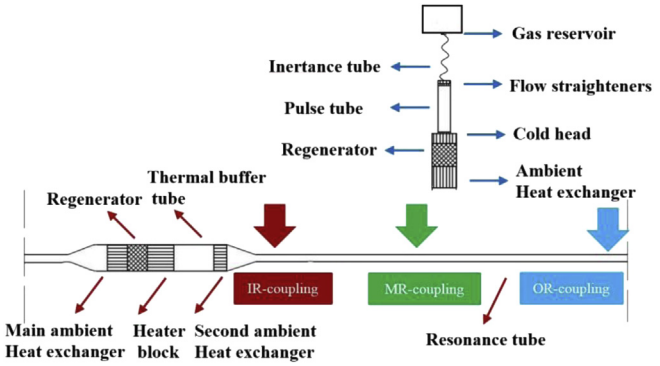

Fig. 2. Enlarged view of one subunit of the acoustically resonant cooling system.

Table 1
Geometrical parameters of the THE and PTC.

THE	Regenerator	80 × 60 (150#)
	Thermal buffer tube	80 × 120
	Heater block	80 × 80
PTC	Regenerator	75 × 70 (300#)
	Pulse tube	37 × 150
	Cold head	75 × 30

Dimensions: inner diameter × length (all in millimeters).

2.2. Numerical model

The simulations were conducted using DeltaEC [12], which is thermoacoustic software that is based on classical thermoacoustic theory [13]. The software provides a series of modules, such as DUCT, HX, STKSCREEN, and STKSCREEN, for the simulation of different thermoacoustic components and systems. Some parameters, such as the gas temperature, pressure amplitude, and phase, are set and initialized by the users. A shooting method is introduced in the software to satisfy the boundary conditions set by the user. A turbulence algorithm is employed for the resonance tube [12]. According to thermoacoustic theory, the momentum, continuity, and energy equations are [13]:

$$\frac{\mathrm{d}p_1}{\mathrm{d}x} = -\frac{\mathrm{i}\omega\rho_m}{1-f_v}\frac{U_1}{A} \tag{1}$$

$$\frac{\mathrm{d}U_1}{\mathrm{d}x} = -\frac{\mathrm{i}\omega A}{\gamma p_m}\left[1+\frac{(\gamma-1)f_\kappa}{1+\xi}\right]p_1 + \frac{(f_\kappa - f_v)}{(1-f_v)(1-\sigma)(1+\xi)}\frac{U_1}{T_m}\frac{\mathrm{d}T_m}{\mathrm{d}x} \tag{2}$$

$$\frac{\mathrm{d}\dot{H}_2}{\mathrm{d}x} = \dot{q} \tag{3}$$

$$\begin{aligned}\dot{H}_2 = {} & \frac{1}{2}\mathrm{Re}\left[p_1\tilde{U}_1\left(1-\frac{f_\kappa-\tilde{f}_v}{(1-f_v)(1-\sigma)(1+\xi)}\right)\right] \\ & + \frac{\rho_m c_p|U_1|^2}{2A\omega(1-\sigma)|1-f_v|^2}\frac{\mathrm{d}T_m}{\mathrm{d}x}\mathrm{Im}\left[\tilde{f}_v + \frac{\left(\tilde{f}_\kappa-\tilde{f}_v\right)(1+\xi f_v/f_\kappa)}{(1+\xi)(1-\sigma)}\right] \\ & - (Ak + A_s k_s)\frac{\mathrm{d}T_m}{\mathrm{d}x}\end{aligned} \tag{4}$$

whereP_1, U_1, H_2, q and $\mathrm{d}T_m/\mathrm{d}x$ are the pressure wave, volume flow rate, total energy flow, heat absorbed or released from/to the heat sinks, and mean temperature gradient, respectively; ω,A,γ,P_m,ρ_m are the angular frequency, cross-sectional area, specific heat ratio, average pressure, and density, respectively; and f_v f_k are viscosity and thermal functions, respectively.

In the calculation, the mean pressure is set as 6 MPa and the heating temperature as 923 K. Generally, the system performance is reflected by two important parameters: the cooling power and total exergy efficiency. To appropriately compare the three coupling positions, the cooling power is set as 750 W at a cooling temperature of 110 K and the total exergy efficiency, defined by

$$\eta_{ex} = \frac{Q_c\left(\frac{T_0}{T_c}-1\right)}{Q_h\left(1-\frac{T_0}{T_h}\right)}, \tag{5}$$

is used as comparison parameter. The temperature of the water-cooled ambient heat exchangers is fixed at 303 K. Owing to the cyclic symmetry of the system, the separating pressure wave and volume flow rates have the same amplitudes and phase differences of 120° at both ends of the sub-unit, so only one subunit needs to be simulated for simplicity.

2.3. Simulation results and discussion

Initially, from a simple viewpoint, coupling of the PTC at the inlet of the resonance tube seems more reasonable because acoustic power can first be utilized by the PTC, rather than be dissipated in the resonance tube. The PTC is therefore primarily designed and optimized for the case of IR-coupling. We initially compared the performances of IR-coupling and OR-coupling, without changing the dimensions listed in Table 1. The resonance tube is 19 mm in diameter and 3 m in length. According to the calculation results, OR-coupling gives exergy efficiency of 14.7% and cooling power of 750 W, while IR-coupling fails to produce any net cooling power at 110 K. As shown in the following sections, when considering different acoustic power transmission characteristics of the resonance tube connected to the PTC at different positions, the dimensions of the resonance tube should be optimized. For the same reason, the impedance of the PTC phase shifter is also optimized to achieve the highest total exergy efficiency according to each connecting position and the dimensions of the resonance tube.

2.3.1. Effects of dimensions of the resonance tube

We first changed the ID (inner diameter) and the length of the resonance tube simultaneously to study the effect of the dimensions of the resonance tube. The simulation results for IR-coupling and OR-coupling are presented in Figs. 3 and 4, respectively. These data show that there is a different optimum length for each tube ID in terms of obtaining the highest total exergy efficiency, although the optimum length is not the same for both couplings. The highest total exergy efficiency of 16.31% can be achieved in OR-coupling using optimal dimensions of a diameter of 27 mm and a length of 3.5 m; this efficiency exceeds the highest total exergy efficiency of 14.93% obtained in IR-coupling with approximately the same resonance tube length.

In subsequent calculations, we kept the length of the resonance tube as optimized at 3.5 m and varied the diameter of the tube. The system performances for IR-coupling, MR-coupling, and OR-coupling are presented in Fig. 5. Note that each curve starts from the tube ID that could give 750 W cooling power at a fixed heating temperature. According to the results, OR-coupling greatly outperforms the other cases for the same ID of the resonance tube.

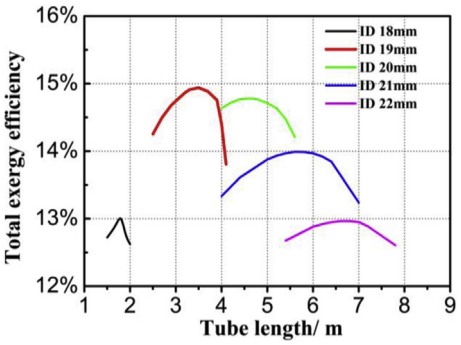

Fig. 3. Dependence of the total exergy efficiency on the dimensions of the resonance tube in IR-coupling.

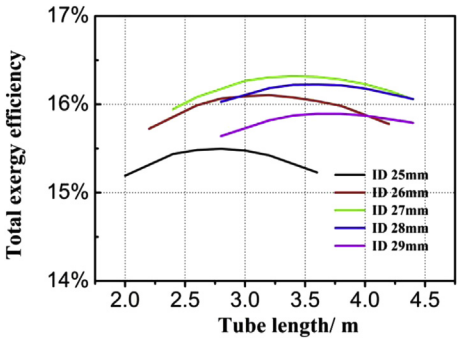

Fig. 4. Dependence of the total exergy efficiency on the dimensions of the resonance tube in OR-coupling.

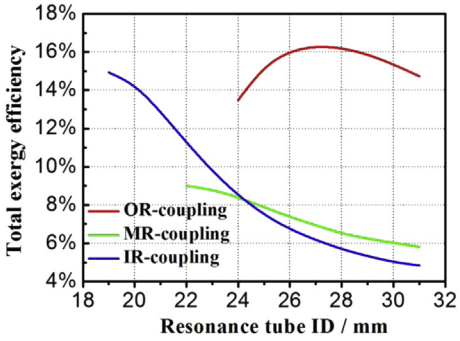

Fig. 5. Dependence of the total exergy efficiency on the inner diameter (ID) of the resonance tube for the three coupling positions. The tube length is 3.5 m.

Taking the ID of 27 mm as an example, an exergy efficiency of 16.3% is achieved in OR-coupling, which greatly exceeds the values of 6.9% in MR-coupling and 6.1% in IR-coupling. For the different tube IDs, MR-coupling has the worst global system performance.

2.3.2. Phase difference analysis

The calculation results reported above led us to further investigate the internal mechanisms and the reasons why OR-coupling achieves better performance. Generally, it is necessary to keep the pressure wave and volume flow rate in phase in the middle of regenerator to obtain high efficiency [14]. Figs. 6 and 7 present the distributions of the phase difference in the THE and PTC for the respective optimal tube IDs for the three coupling cases. In the THE, the x-axis begins at the main water-cooled ambient heat exchanger and extends to the regenerator, heater block, thermal buffer tube, secondary water-cooled ambient heat exchanger, and finally, to the

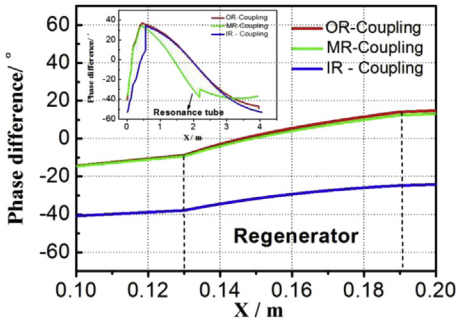

Fig. 6. Phase difference between the pressure wave and volume flow rate in the thermoacoustic heat engine (THE).

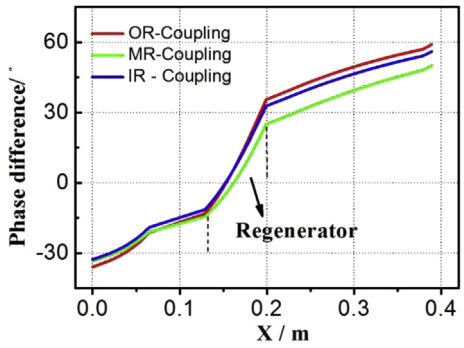

Fig. 7. Phase difference between the pressure wave and volume flow rate in the pulse tube cooler (PTC).

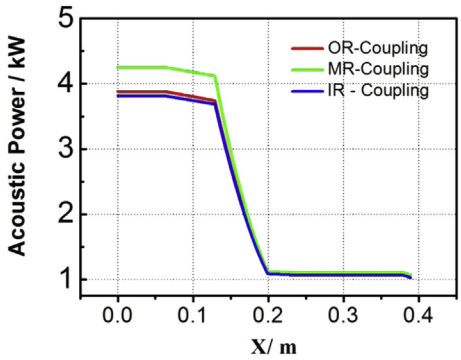

Fig. 9. Acoustic power distribution in the PTC.

resonance tube. In the PTC, the x-axis begins at the water-cooled ambient heat exchanger, and extends to the regenerator, cold head, pulse tube, and finally, to the flow straighteners. The phase shifter of the PTC (the inertance tube and gas reservoir) is taken as a lumped acoustical impedance. In the THE regenerator, the phase difference in IR-coupling varies from −38.9 to −24.7°, indicating that the acoustic field in the regenerator somehow deviates from the traveling-wave field. In the other two cases, the phase difference distributions inside the THE regenerator are similar and both pass through zero degrees, which means that a reasonable acoustic field is provided. In the PTC regenerator, the phase difference distributions are close to each other and all achieve an in-phase relationship.

Taking a closer look at the situation for each coupling position, the phase difference before and after the connecting position of the THE changes significantly in IR-coupling (from 9.3 to 34.2°) but only minimally in MR-coupling (from −38 to −29.7°) and OR-coupling (from −47.1 to −49.3°). The phases at the branch of the PTC are −32.8, −33.4, and −36.5° in IR-coupling, MR-coupling, and OR-coupling, respectively. With reference to the small subplot in Fig. 6, phase difference at the PTC inlet has the same sign as that at the middle or outlet of the resonance tube, while it has a different sign to that at the inlet of the resonance tube. From the viewpoint of phasor analysis, connecting the PTC at the resonance tube inlet will exert a greater influence on the local acoustic field.

2.3.3. Distribution of acoustic power

Distributions of the acoustic power in the THE and PTC are shown in Figs. 8 and 9, respectively. The acoustic power transmission in the resonance tube depends on the coupling position: in the case of IR-coupling, much of the acoustic power generated in the regenerator is first consumed by the PTC, and the remainder passes through the resonance tube to the next subunit; in the case of MR-coupling, after dissipation in the first half of the resonance tube, part of the acoustic power goes to the PTC and the remainder goes through the second half of the resonance tube; in the case of OR-coupling, the acoustic power is first consumed by the resonance tube, and then partly consumed by the PTC and partly delivered to the latter subunit. The calculation results reveal that the THE can provide the PTC with net acoustic power of 3815 W, 4252 W, and 3882 W in IR-coupling, MR-coupling, and OR-coupling, corresponding to THE exergy efficiencies of 43.2%, 29.1%, and 48.1%, respectively. The THE obviously performs poorly in the case of MR-coupling. A closer look reveals that a large amount of acoustic power dissipated in the resonance tube, which leads to the low efficiency of the THE. The acoustic power entering the PTC is mainly consumed by the PTC regenerator to pump heat from the cold head. In IR-coupling, MR-coupling, and OR-coupling, the exergy efficiencies of the PTC are 34.5%, 30.9%, and 33.9%, respectively.

2.3.4. Analysis of exergy loss

High exergy losses in the main components can directly degrade the system efficiency and should be considered in further investigations. The exergy loss ratio studied here is defined as the exergy loss divided by the input heat exergy (i.e, $Q_H(1 - T_0/T_H)$, where Q_H is the input heating power, T_0 is the temperature of the surrounds, and T_H is the heating temperature).

Fig. 10 shows the exergy loss ratios in some of the main components for the three coupling positions. In all cases, the largest portion of total exergy loss is attributed to the resonance tube, followed by losses in the PTC regenerator, the THE regenerator, and the phase shifter of the PTC. To realize a highly efficient cooling system, the exergy loss in the resonance tube should therefore be reduced as much as possible and the exergy losses in other components should also be limited. For MR-coupling, the exergy loss ratio of the resonance tube is 38.9%, while for IR-coupling and OR-

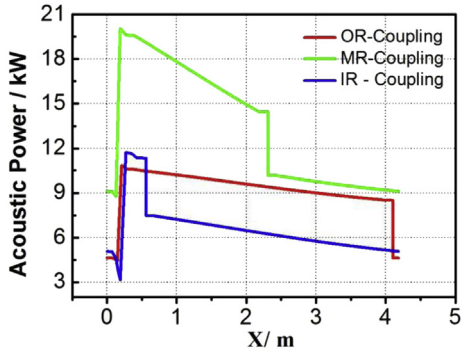

Fig. 8. Acoustic power distribution in the THE.

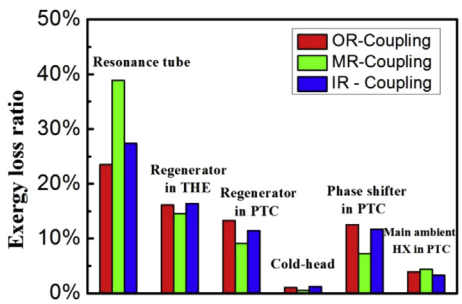

Fig. 10. Comparison of the exergy loss ratio in main components.

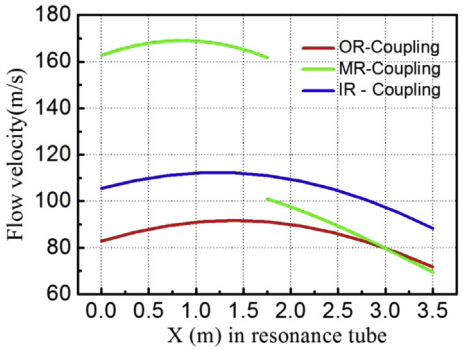

Fig. 11. Flow velocity distributions in the resonance tube.

coupling, the exergy loss ratios are only 27.4% and 23.5%, respectively. This can be explained by the flow velocity distributions in the resonance tube presented in Fig. 11. In this figure, the x-axis begins at the inlet of the resonance tube and extends to the outlet of the resonance tube. It is seen that the flow velocity in the case of OR-coupling is lower than that of other cases. This is mainly because the enlarged ID of the resonance tube leads to low velocities, thus reducing the viscosity losses. For MR-coupling, in the first half of the resonance tube, the flow velocity is very high, at almost twice the velocity for OR-coupling. This has an appreciable negative effect on the system performance. In the second half of the resonance tube, the velocity in the case of MR-coupling falls between the values for OR-coupling and IR-coupling, which is acceptable.

3. Conclusions

The coupling characteristics of a looped three-stage thermoacoustically-driven PTC are investigated in this paper. The results of the study are summarized as follows:

i) System performances for three representative coupling positions (inlet, middle, and outlet) of the resonance tube are compared and analyzed numerically. In all three cases, the system performances show strong but different dependences on the dimensions of the resonance tube. Employing the optimal resonance tube for each position, the highest total exergy efficiency of 16.3% is obtained for OR-coupling, which is better than the values of 14.93% for IR-coupling and 9% obtained for MR-coupling.

ii) The superior performance of OR-coupling can be explained in two ways: on one hand, the phase relationship in the branch of the THE strongly conforms to the demand at the inlet of the PTC, and a satisfying phase relationship is thus achieved; on the other hand, the enlarged diameter of the resonance tube reduces the flow velocity, and thus the exergy loss due to viscosity resistance.

iii) The worst global performance is observed for MR-coupling, mainly because of the high flow velocity in the first half of the resonance tube which results in a large exergy loss in the resonance tube.

In the near future, experiments will be conducted to verify these simulation results.

Acknowledgment

This work was financially supported by the Natural Sciences Foundation under contract numbers 51276187 and U1137606.

References

[1] Radebaugh R, McDermott KM, Swift GW, Martin RA. Development of a thermoacoustically driven orifice pulse tube refrigerator. In: Proceedings of the interagency meeting on cryocoolers. Plymouth, MA; 1990. p. 205–20.
[2] Dai W, Luo EC, Hu JY, Ling H. A heat-driven thermoacoustic cooler capable of reaching liquid nitrogen temperature. Appl Phys Lett 2005;86:224103.
[3] Hu JY, Dai W, Luo EC. Thermoacoustic driven pulse tube coolers with acoustic amplifier. Adv Cryog Eng 2006;51:1564–71.
[4] Hu JY, Luo EC, Dai W, Zhou Y. A heat-driven thermoacoustic cryocooler capable of reaching below liquid hydrogen temperature. Chin Sci Bull 2007;52(4):574–6.
[5] Tang K, Bao R, Cheng GB, Qiu Y, Shou L, Huang ZJ, et al. Thermoacoustically driven pulse tube cooler below 60 K. Cryogenics 2007;47:526–9.
[6] Kees DB. Novel 4-stage traveling wave thermoacoustic power generator. In: International conference on nanochannels and minichannels; 2010.
[7] Li DH, Chen YY, Luo EC, Wu ZH. Study of a liquid-piston traveling-wave thermoacoustic heat engine with different working gases. Energy 2014;74:158–63.
[8] Wu ZH, Yu GY, Zhang LM, Dai W, Luo EC. Development of a 3 kW double-acting thermoacoustic Stirling electric generator. Appl Energy 2014;136:866–72.
[9] Xu JY, Yu GY, Zhang LM, Dai W, Luo EC. Numerical investigation on a 300 Hz pulse tube cryocooler driven by a three-stage traveling-wave thermoacoustic heat engine. Cryogenics 2015;71:68–75.
[10] Tong H, Hu JY, Zhang LM, Luo EC. Experimental study of an acoustic resonant cooling system. Phys Procedia 2015;67:445–50.
[11] Zhang LM, Hu JY, Wu ZH, Luo EC, Xu JY, Bi TJ. A 1 kW-class multi-stage heat-driven thermoacoustic cryocooler system operating at liquefied natural gas temperature range. Appl Phys Lett 2015;107:033905.
[12] Ward B, Clark J, Swift G. Design environment for low-amplitude thermoacoustic energy conversion, DELTAEC version 6.2 users Guide. Los Alamos, the US: Los Alamos National Laboratory; 2008.
[13] Swift GW. Thermoacoustics: a unifying perspective for some engines and refrigerators. New York: AIP Press; 2002.
[14] Radebaugh R. Development of the pulse tube refrigerator as an efficient and reliable cooler. In: Proc institute of refrigeration, London, vol. 96; 1999–2000. p. 11–31.